

# Self-learning sparse PCA for multimode process monitoring

Jingxin Zhang, Donghua Zhou, *Fellow, IEEE*, and Maoyin Chen, *Member, IEEE*

**Abstract**—This paper proposes a novel sparse principal component analysis algorithm with self-learning ability for successive modes, where synaptic intelligence is employed to measure the importance of variables and a regularization term is added to preserve the learned knowledge of previous modes. Different from traditional multimode monitoring methods, the monitoring model is updated based on the current model and new data when a new mode arrives, thus delivering prominent performance for sequential modes. Besides, the computation and storage resources are saved in the long run, because it is not necessary to retrain the model from scratch frequently and store data from previous modes. More importantly, the model furnishes excellent interpretability owing to the sparsity of parameters. Finally, a numerical case and a practical pulverizing system are adopted to illustrate the effectiveness of the proposed algorithm.

**Index Terms**—Multimode process monitoring, sparse PCA, synaptic intelligence, self-learning

## I. BACKGROUND

Multimode process monitoring is increasingly demanded and significant, as industrial systems generally operate in varying modes due to raw materials, changing load, etc [1]–[3]. Data from different modes have different characteristics, such as mean value and variance [4], [5]. It is imperative to investigate the effective manners for multimode processes [6], [7].

Marcos *et al* [1] summarized the techniques for multimode processes and divided the methods into two major categories, namely, single-model schemes and multiple-model schemes. Single-model methods aim to find a transformation to remove the multimodality features and then the fault is detected by a decision function [3]. Multiple-model methods identify the mode and build the monitoring model within each mode [2], [8], [9]. However, the information on all modes should be complete, which is evidently impossible in real systems. When a new mode arrives, the learned knowledge of previous modes may be overwritten when training the same monitoring

model for the current mode, which would lead to a abrupt performance decrease. This phenomenon has been analyzed and discussed in [10]. Overall, state-of-the-art methods aforementioned need to retrain the monitoring model from scratch [10], [11].

Since the operating modes in practical systems appear successively, it is consuming to progressively retain massive data and repeatedly retrain the models. Therefore, it is important to establish a self-learning monitoring model and update it continually when a new mode arrives. One strategy of realizing self-learning ability is continual learning, where the model is updated when new data are available. The technical core of continual learning is to accommodate new information while preserving the acquired knowledge [11], [12]. However, there exists one longstanding challenge, namely, ‘catastrophic forgetting’ issue, where the information of previous modes is overlapped by new data and a new model based on new data may fail to monitor previous modes. Various schemes have been developed to alleviate this issue and supply excellent performance [11]–[14]. Nevertheless, it is still scarce to investigate the process monitoring techniques with self-learning ability [15]–[17].

Zhang *et al* firstly focused on this research and illustrated the necessity in [10], where a single monitoring model with continual learning ability was investigated for successive modes. Elastic weight consolidation (EWC) [11] was employed to solve the ‘catastrophic forgetting’ of traditional principal component analysis (PCA) [10], [18], referred to as PCA-EWC, which retained the significant information of previous modes by slowing down the changes of certain influential parameters. Note that EWC estimates the importance measure offline based on the point estimate of Fisher information matrix (FIM) [11].

Consider the poor interpretability of PCA, this paper investigates sparse PCA (SPCA) with self-learning ability for multimode process monitoring, where the model is updated based on the current model and new data. Instead of EWC, we consider synaptic intelligence (SI), which calculates the importance matrix along the entire learning trajectory [19]–[21], by computing the gradients of loss and the parameter update. For convenience, the proposed SPCA with SI is denoted as SPCA-SI. Compared with PCA-EWC [10], SPCA-SI utilizes  $L_1$  regularization to enhance the sparsity of critical parameters, thus providing better model interpretability. Besides, the importance measure by SI is easier to estimate than EWC, because the gradients are usually available while FIM is intractable. Moreover, sparse representation is also beneficial to reduce catastrophic forgetting, as there are fewer model-

This work was supported by National Natural Science Foundation of China [grant numbers 62033008, 61873143]. (Corresponding authors: Donghua Zhou; Maoyin Chen)

Jingxin Zhang is with the Department of Automation, Tsinghua University, Beijing 100084, China (e-mail: zjx18@mails.tsinghua.edu.cn).

Donghua Zhou is with College of Electrical Engineering and Automation, Shandong University of Science and Technology, Qingdao 266000, China and also with the Department of Automation, Tsinghua University, Beijing 100084, China (e-mail: zdh@mail.tsinghua.edu.cn).

Maoyin Chen is with the Department of Automation, Tsinghua University, Beijing 100001, China and also with School of Automation and Electrical Engineering, Linyi University, Linyi 276005, China (e-mail: mychen@tsinghua.edu.cn).

This paper has been submitted for IEEE Transactions on Industrial Informatics for potential publication.

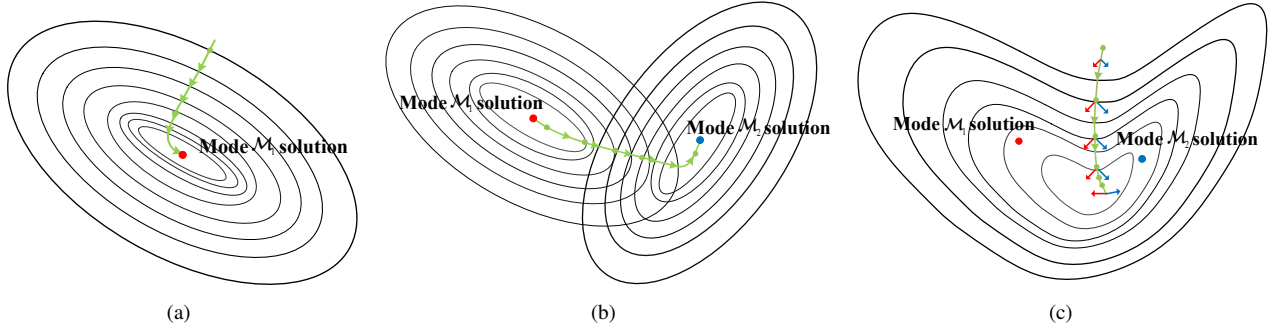


Fig. 1. Illustration of gradient decent optimization for different modes: (a) The trajectory for one mode; (b) The trajectory when training the same model on the second mode subsequently; (c) The trajectory when minimizing the total loss from both modes (green) and gradients from each mode (red and blue) [13].

sensitive parameters [13], [14], [20]. In this paper, we assume that the mode transition is accomplished in a short time and the switching time is available.

The rest of this paper is organized below. Section II reviews SPCA and SI briefly, and introduces the research problem. The proposed SPCA-SI algorithm is elaborated in Section III and settled by accelerated proximal gradient descent (APG) method. A novel  $T^2$  statistic is proposed and the monitoring procedure is summarized in Section IV. Besides, the influence of parameters and computational complexity are discussed. The effectiveness of the proposed approach is illustrated by a numerical case study and a practical coal puzzling system in Section V. The concluding remark is given in Section VI.

## II. PRELIMINARY

### A. Revisit of SPCA

Here we give another perspective of SPCA, where the projection vectors are acquired one by one.

Given the dataset  $\mathbf{X} \in R^{N \times m}$ ,  $N$  is the number of samples and  $m$  is the number of variables. PCA aims to minimize the reconstruction error, namely,

$$\begin{aligned} \min \quad & \|\mathbf{X} - \mathbf{X}\mathbf{p}\mathbf{p}^T\|_F^2 \\ \text{s.t.} \quad & \mathbf{p}^T\mathbf{p} = 1 \end{aligned}$$

where  $\mathbf{p} \in R^m$  is the projection vector.

Consider the virtues of sparsity,  $L_1$  regularization is adopted to enhance interpretability and alleviate catastrophic forgetting simultaneously [13], [14]. Thus, the objective of SPCA is

$$\begin{aligned} \min \quad & \|\mathbf{X} - \mathbf{X}\mathbf{p}\mathbf{p}^T\|_F^2 + \lambda \|\mathbf{p}\|_1 \\ \text{s.t.} \quad & \mathbf{p}^T\mathbf{p} = 1 \end{aligned} \quad (1)$$

where  $\lambda$  is a regularization parameter. After  $\mathbf{p}$  is calculated, let  $\mathbf{X} = \mathbf{X} - \mathbf{X}\mathbf{p}\mathbf{p}^T$ , and repeat (1) until  $l$  projection vectors are obtained. Here, the number of principal components  $l$  is determined by cumulative percent variance.

### B. Review of SI

The synaptic framework was proposed and detailed information has been described in [19]. Here we overview the key points [19], [20].

For a learning process, we aim to seek for the optimal parameter  $\theta$  given the objective function  $J(\theta)$ . Gradient-based

methods are effective manners to solve the optimization problem. SI estimates the importance measure for each parameter along the learning trajectory, which reflects the sensitivity of each parameter to the loss.

The gradient is a conservative field, and the value of the integral along the trajectory is equal to the difference between the end point and the start point [19]. Consider an infinitesimal parameter update  $\delta(k)$  at  $k$ th iteration, the change in loss is approximated by

$$J(\theta(k) + \delta(k)) - J(\theta(k)) \approx \sum_i g_i(k) \delta_i(k)$$

where  $\mathbf{g} = \frac{\partial J}{\partial \theta}$  is the gradient,  $\delta_i(k) = \theta_i(k) - \theta_i(k-1)$ . During the whole learning process, the change in loss over the entire trajectory is calculated by

$$\begin{aligned} \sum_k \mathbf{g}(k) \delta(k) &= \sum_i \sum_k g_i(k) \delta_i(k) \\ &= - \sum_i \varpi_i \end{aligned}$$

More intuitively [21],

$$\varpi_i = \sum_k (\theta_i(k) - \theta_i(k-1)) \frac{-\partial J}{\partial \theta_i(k)} \quad (2)$$

Then, the importance measure is normalized by [20]

$$\bar{\varpi}_i = \max\left(0, \frac{\varpi_i}{(\Delta\theta_i)^2 + \zeta}\right) \quad (3)$$

thus the regularization term and the loss shares the same unit.  $\Delta\theta_i = \sum_k (\theta_i(k) - \theta_i(k-1))$  is the total change for each parameter and  $\zeta$  is added to avoid ill-conditioning issue.

### C. Problem reformulation

This paper proposes a self-learning process monitoring approach for successive modes, which is built based on SPCA and the model is updated when a new mode arrives. We take two modes to depict the research problem by Fig. 1 [13].

When training the monitoring model for mode  $\mathcal{M}_1$ , the optimization issue is settled by gradient decent method and the trajectory of SPCA is exhibited in Fig. 1a. When a new mode  $\mathcal{M}_2$  arrives, traditional SPCA-based methods generally train the model subsequently, as illustrated in Fig. 1b. In this case, the learning of mode  $\mathcal{M}_2$  leads to an overlap of the

learned knowledge, which indicates that the retrained model is not efficient for the previous mode  $\mathcal{M}_1$ . This paper aims to accommodate new data by a continually updated model while accumulating the learned knowledge, thus delivering brilliant performance for two or more modes. As shown in Fig. 1c, the total loss for both modes is considered simultaneously and the optimal solution is an equilibrium between the gradients of different modes [13].

### III. METHODOLOGY

In this section, we present the procedure of SPCA-SI for the first mode and the objective is optimized by APG. Then, SPCA-SI is extended to more general cases.

#### A. SPCA-SI for the first mode

For the first mode  $\mathcal{M}_1$ , data  $\mathbf{X}_1$  are collected. We settle the issue (1) by augmented Lagrangian function:

$$J = \|\mathbf{X}_1 - \mathbf{X}_1 \mathbf{p} \mathbf{p}^T\|_F^2 + \lambda \|\mathbf{p}\|_1 + \mu (\mathbf{p}^T \mathbf{p} - 1)^2 \quad (4)$$

where  $\mu$  is the Lagrange parameter. (4) is nonconvex and nonsmooth, and can not be directly settled by gradient-based methods.

APG is an effective technique to deal with this type of optimization issue and employed in this paper [22]. We divide (4) into smooth part  $g(\mathbf{p})$  and nonsmooth part  $h(\mathbf{p})$ , namely,

$$g(\mathbf{p}) = \|\mathbf{X}_1 - \mathbf{X}_1 \mathbf{p} \mathbf{p}^T\|_F^2 + \mu (\mathbf{p}^T \mathbf{p} - 1)^2 \quad (5)$$

$$h(\mathbf{p}) = \lambda \|\mathbf{p}\|_1 \quad (6)$$

#### B. Solution with APG

The procedure of APG contains the gradient-based part of  $g(\mathbf{p})$  and the proximal gradient.

For the smooth part  $g(\mathbf{p})$ , (5) is equivalent to

$$g(\mathbf{p}) = \text{tr}(\mathbf{X}_1^T \mathbf{X}_1) + \mu + \text{tr}(\mathbf{p} \mathbf{p}^T (\mathbf{X}_1^T \mathbf{X}_1 + \mu \mathbf{I}) \mathbf{p} \mathbf{p}^T) - 2 \text{tr}(\mathbf{p} \mathbf{p}^T (\mathbf{X}_1^T \mathbf{X}_1 + \mu \mathbf{I}))$$

Thus, the gradients are

$$\nabla_{\mathbf{p}} g(\mathbf{p}) = \frac{\partial g}{\partial \mathbf{p}} = \mathbf{p} \mathbf{p}^T \mathbf{G}_1 \mathbf{p} + \mathbf{G}_1 \mathbf{p} \mathbf{p}^T \mathbf{p} - 2 \mathbf{G}_1 \mathbf{p} \quad (7)$$

$$\nabla_{\mu} g(\mathbf{p}) = \frac{\partial g}{\partial \mu} = (\mathbf{p}^T \mathbf{p} - 1)^2 \quad (8)$$

where  $\mathbf{G}_1 = 2(\mathbf{X}_1^T \mathbf{X}_1 + \mu \mathbf{I})$ .

For  $h(\mathbf{p})$ , the proximal function is defined as [22], [23]

$$\mathbf{p}^+ = \arg \min_{\mathbf{z}} \frac{1}{2t} \|\mathbf{z} - (\mathbf{p} - t \nabla_{\mathbf{p}} g(\mathbf{p}))\|_2^2 + h(\mathbf{z}) \quad (9)$$

$$:= \text{prox}_{h,t}(\mathbf{p} - t \nabla_{\mathbf{p}} g(\mathbf{p}))$$

Inspired by Adam [24], the learning rate  $t$  is adaptively estimated to accelerate convergence. At  $k$ th iteration,  $t_k$  is calculated by

$$t_k = f(\alpha, t_{k-1}, \nabla_{\mathbf{p}} g_k)$$

$$= \alpha / \left( \sqrt{(\tau_2 t_{k-1} + (1 - \tau_1) \|\nabla_{\mathbf{p}} g_k\|^2)} / (1 - \tau_2) + \varepsilon \right) \quad (10)$$

---

#### Algorithm 1 APG for optimization issue (4)

---

**Input:** Initialize  $\mathbf{p}_1 = \mathbf{p}_0$ ,  $\mathbf{z}_1 = \mathbf{p}_0$ ,  $t_1 = t_0 = 0$ ,  $\bar{\omega}_1 = \mathbf{0}$ ,  $\tau_1 = 0.9$ ,  $\tau_2 = 0.999$ ,  $\varepsilon = 10^{-8}$ ,  $t_0^y = 10^{-4}$ ,  $t_0^p = 10^{-4}$ ,  $t_0^\mu = 10^{-4}$ ,  $\alpha^p = 0.001$ ,  $\alpha^\mu = 0.01$

**Output:** the optimal  $\mathbf{p}$ , and the importance measure  $\omega$   
**for**  $k = 1, 2, 3, \dots$  **do**

1) Update the projection vector:

$$\text{a) } \mathbf{y}_k = \mathbf{p}_k + \frac{t_{k-1}}{t_k} (\mathbf{z}_k - \mathbf{p}_k) + \frac{t_{k-1}-1}{t_k} (\mathbf{p}_k - \mathbf{p}_{k-1})$$

$$\text{b) } \mathbf{z}_{k+1} = \text{prox}_{h,t^y}(\mathbf{y}_k - t_k^y \nabla_{\mathbf{p}} g(\mathbf{y}_k)), \text{ calculate } t_k^y = f(\alpha^p, t_{k-1}^y, \nabla_{\mathbf{p}} g(\mathbf{y}_k)) \text{ by (10)}$$

$$\text{c) } \mathbf{v}_{k+1} = \text{prox}_{h,t^p}(\mathbf{p}_k - t_k^p \nabla_{\mathbf{p}} g(\mathbf{p}_k)), \text{ calculate } t_k^p = f(\alpha^p, t_{k-1}^p, \nabla_{\mathbf{p}} g(\mathbf{p}_k)) \text{ by (10)}$$

$$\text{d) } t_{k+1} = \frac{\sqrt{4(t_k)^2 + 1} + 1}{2}$$

$$\text{e) } \mathbf{p}_{k+1} = \begin{cases} \mathbf{z}_{k+1}, & \text{if } J(\mathbf{z}_{k+1}) \leq J(\mathbf{v}_{k+1}) \\ \mathbf{v}_{k+1}, & \text{otherwise} \end{cases}$$

2) Update  $\mu$ ,  $\mu_{k+1} = \mu_k + t_k^\mu \nabla_{\mu} g(\mathbf{p}_{k+1})$ ,  $t_k^\mu = f(\alpha^\mu, t_{k-1}^\mu, \nabla_{\mu} g(\mathbf{p}_{k+1}))$

3) Calculate the importance measure  $\bar{\omega}_{k+1} = \bar{\omega}_k - ((\nabla g(\mathbf{p}_{k+1}))^T \odot (\mathbf{p}_{k+1} - \mathbf{p}_k)^T)^T$

**end for**

Normalize  $\bar{\omega}$  by (13) and denote as  $\omega$

---

where  $\nabla g_k$  is the corresponding gradient.  $\alpha$ ,  $\tau_1$  and  $\tau_2$  are constants.  $\varepsilon$  is added to avoid ill-conditioning issue.

The proximal function  $\text{prox}$  is defined and the proximal gradient is calculated by the soft threshold [22]

$$\text{prox}_{h,t}(\mathbf{p}) = \arg \min_{\mathbf{z}} \frac{1}{2t} \|\mathbf{z} - \mathbf{p}\|_2^2 + \lambda \|\mathbf{z}\|_1$$

$$= S_{\lambda t}(\mathbf{p})$$

The soft threshold  $S_{\lambda t}(\mathbf{p})$  has an analytical solution [25]:

$$[S_{\lambda t}]_i = \begin{cases} p_i - \lambda t, & p_i > \lambda t \\ 0, & |p_i| \leq \lambda t \\ p_i + \lambda t, & p_i < -\lambda t \end{cases} \quad (11)$$

where  $p_i$  is the  $i$ th element of  $\mathbf{p}$ .

According to (2), the importance measure is computed by

$$\bar{\omega} = \sum_k \left( (\nabla g(\mathbf{p}_k))^T \odot (\mathbf{p}_k - \mathbf{p}_{k-1})^T \right)^T \quad (12)$$

where  $\odot$  denotes the Khatri-Rao product and  $\mathbf{p}_k$  is the projection vector at  $k$ th iteration step. Accordingly, each element of  $\bar{\omega}$  is normalized by

$$\omega_i = \max \left( 0, \frac{\bar{\omega}_i}{(\Delta p_i)^2 + \zeta} \right) \quad (13)$$

where  $\Delta p_i$  represents the total change,  $1 \leq i \leq m$ . The solution is summarized in Algorithm 1.

The procedure of SPCA-SI is summarized in Algorithm 2. For convenience, the optimal projection matrix and the importance measure are denoted as  $\mathbf{P}_{\mathcal{M}_1}$  and  $\Omega_{\mathcal{M}_1}$ , respectively.

#### C. SPCA-SI for multiple modes

When the mode  $\mathcal{M}_i$  ( $i \geq 2$ ) arrives, only data  $\mathbf{X}_i$  are available for training and data from previous modes are not

retained. SPCA-SI aims to learn the new mode while consolidating the acquired knowledge of previous modes. As shown in Fig. 1c, we need to minimize the total loss of all modes, with the constraint that the loss functions of previous trained modes are unavailable. To alleviate catastrophic forgetting, drastic changes to influential parameters in the past should be avoided. Therefore, a quadratic surrogate loss is introduced to approximate the total loss of previous modes [19].

The model of SPCA-SI is updated based on the current model and new data. For the  $j$ th projection vector ( $1 \leq j \leq l$ ), the objective is designed as:

$$\begin{aligned} \min \quad & \| \mathbf{X}_i - \mathbf{X}_i \mathbf{p} \mathbf{p}^T \|_F^2 + \left( \mathbf{p} - \mathbf{p}_{\mathcal{M}_{i-1}} \right)^T \bar{\Omega} \left( \mathbf{p} - \mathbf{p}_{\mathcal{M}_{i-1}} \right) \\ & + \lambda \|\mathbf{p}\|_1 \\ \text{s.t.} \quad & \mathbf{p}^T \mathbf{p} = 1 \end{aligned} \quad (14)$$

where  $\mathbf{p}_{\mathcal{M}_{i-1}}$  is the  $j$ th column of  $\mathbf{P}_{\mathcal{M}_{i-1}}$ ,  $\bar{\Omega} = \gamma_i \text{diag}(\boldsymbol{\omega})$ ,  $\boldsymbol{\omega}$  is the importance measure corresponding to  $\mathbf{p}_{\mathcal{M}_{i-1}}$  and the  $j$ th column of  $\bar{\Omega}_{\mathcal{M}_{i-1}}$ ,  $\bar{\Omega}_{\mathcal{M}_{i-1}} = \sum_{r=1}^{i-1} \Omega_{\mathcal{M}_r}$ , and  $\gamma_i$  is the weight which trades off previous versus current modes. Similar to [11], [19], the additional regularization term is the quadratic surrogate loss, which makes the optimal parameters of current mode close to the previous one, with a small loss.

Similarly, the augmented Lagrangian function is depicted as

$$\begin{aligned} J = & \| \mathbf{X}_i - \mathbf{X}_i \mathbf{p} \mathbf{p}^T \|_F^2 + \lambda \|\mathbf{p}\|_1 + \mu (\mathbf{p}^T \mathbf{p} - 1)^2 \\ & + \left( \mathbf{p} - \mathbf{p}_{\mathcal{M}_{i-1}} \right)^T \bar{\Omega} \left( \mathbf{p} - \mathbf{p}_{\mathcal{M}_{i-1}} \right) \end{aligned} \quad (15)$$

The smooth part  $g(\mathbf{p})$  and the corresponding gradient are

$$\begin{aligned} g(\mathbf{p}) = & \| \mathbf{X}_i - \mathbf{X}_i \mathbf{p} \mathbf{p}^T \|_F^2 + \left( \mathbf{p} - \mathbf{p}_{\mathcal{M}_{i-1}} \right)^T \bar{\Omega} \left( \mathbf{p} - \mathbf{p}_{\mathcal{M}_{i-1}} \right) \\ & + \mu (\mathbf{p}^T \mathbf{p} - 1)^2 \end{aligned} \quad (16)$$

$$\nabla_{\mathbf{p}} g(\mathbf{p}) = \mathbf{p} \mathbf{p}^T \mathbf{G}_i \mathbf{p} + \mathbf{G}_i \mathbf{p} \mathbf{p}^T \mathbf{p} - 2 \mathbf{G}_i \mathbf{p} + 2 \bar{\Omega} \left( \mathbf{p} - \mathbf{p}_{\mathcal{M}_{i-1}} \right) \quad (17)$$

where  $\mathbf{G}_i = 2 \left( \mathbf{X}_i^T \mathbf{X}_i + \mu \mathbf{I} \right)$ .

The solution can refer to Algorithm 2. The optimization problem is (15), and the gradients are calculated by (17) and (8). The optimal projection matrix and importance measure are denoted as  $\mathbf{P}_{\mathcal{M}_i}$  and  $\Omega_{\mathcal{M}_i}$ , respectively.

---

#### Algorithm 2 Procedure of SPCA-SI

---

**Require:** data  $\mathbf{X}$ ,  $l$

**Ensure:** The projection matrix  $\mathbf{P}$ , the importance measure  $\Omega$

- 1: Initialize  $\mathbf{P}^0 = [ \mathbf{p}_1^0 \ \cdots \ \mathbf{p}_l^0 ] = \mathbf{I}_{m,l}$ ,  $j = 1$ ;
  - 2: Scale  $\mathbf{X}$  to zero mean and unit variance;
  - 3: Let  $\mathbf{p}_0 = \mathbf{p}_j^0$ , solve (4) by APG as summarized in Algorithm 1. The gradients are calculated by (7-8);
  - 4: The optimal projection vector and importance measure are denoted as  $\mathbf{p}_j$  and  $\omega_j$ . Deflate  $\mathbf{X}$  as  $\mathbf{X} := \mathbf{X} - \mathbf{X} \mathbf{p}_j \mathbf{p}_j^T$ ;
  - 5: Let  $j = j + 1$ , return to step 3 until  $j > l$ ;
  - 6:  $\mathbf{P} = [ \mathbf{p}_1 \ \cdots \ \mathbf{p}_l ]$ ,  $\Omega = [ \omega_1 \ \cdots \ \omega_l ]$ .
- 

---

#### Algorithm 3 Off-line training phase of SPCA-SI

---

- 1: For the mode  $\mathcal{M}_1$ , collect data  $\mathbf{X}_1$ ;
  - 2: Normalize  $\mathbf{X}_1$  to zero mean and unit variance;
  - 3: Perform traditional PCA on  $\mathbf{X}_1$  and calculate the number of principal components  $l$ ;
  - 4: Solve the issue (4) by Algorithm 2, acquire  $\mathbf{P}_{\mathcal{M}_1}$  and  $\Omega_{\mathcal{M}_1}$ . The gradients are calculated by (7-8);
  - 5: Calculate statistics by (18-19) and thresholds by KDE;
  - 6: For the mode  $\mathcal{M}_i$  ( $i \geq 2$ ), collect data  $\mathbf{X}_i$ ;
  - 7: Scale  $\mathbf{X}_i$  to zero mean and unit variance;
  - 8: Solve the issue (15) by Algorithm 2, acquire  $\mathbf{P}_{\mathcal{M}_i}$  and  $\Omega_{\mathcal{M}_i}$ . The gradients are calculated by (8) and (17);
  - 9: Calculate statistics by (18-19) and thresholds by KDE.
- 

## IV. MONITORING MODEL AND DISCUSSION

### A. Monitoring statistics

Two statistics are designed to monitor the operating condition. To enhance the monitoring performance for previous modes, the partial covariance information of last mode is adopted to calculate  $T^2$  statistic. For mode  $\mathcal{M}_i$  ( $i \geq 1$ ),

$$T^2 = \mathbf{x}^T \mathbf{P}_{\mathcal{M}_i} \Xi_{\mathcal{M}_i}^{-1} \mathbf{P}_{\mathcal{M}_i}^T \mathbf{x} \quad (18)$$

where  $\mathbf{x} \in \mathbf{X}_i$ ,  $\mathbf{P}_{\mathcal{M}_i}$  is the projection matrix,  $\Xi_{\mathcal{M}_i} = \mathbf{P}_{\mathcal{M}_i}^T \left( \eta \frac{\mathbf{X}_i^T \mathbf{X}_i}{N_i - 1} + (1 - \eta) \mathbf{P}_{\mathcal{M}_{i-1}} \Xi_{\mathcal{M}_{i-1}} \mathbf{P}_{\mathcal{M}_{i-1}}^T \right) \mathbf{P}_{\mathcal{M}_i}$ , and  $N_i$  is the number of samples,  $\eta$  trades off the previous versus current modes with  $0 \leq \eta \leq 1$ .  $\mathbf{P}_{\mathcal{M}_{i-1}}$  and  $\Xi_{\mathcal{M}_{i-1}}$  are acquired from mode  $\mathcal{M}_{i-1}$ , which represent the information of previous modes without storing the original data. When  $i = 1$ , let  $\eta = 1$ ,  $\Xi_{\mathcal{M}_1} = \frac{\mathbf{X}_1^T \mathbf{X}_1}{N_1 - 1}$ . If  $i > 1$ ,  $\eta$  is estimated by the importance of previous modes. Correspondingly, the squared prediction error (SPE) is calculated by

$$SPE = \mathbf{x}^T \left( \mathbf{I} - \mathbf{P}_{\mathcal{M}_i} \mathbf{P}_{\mathcal{M}_i}^T \right) \mathbf{x} \quad (19)$$

The thresholds are calculated by kernel density estimation (KDE) [26] and the confidence level is 99%. Once one statistic is beyond its threshold, a fault is detected. The training procedure is summarized in Algorithm 3.

### B. Discussion

1) *Parameter setting:* SPCA-SI has three regularization parameters.  $\lambda$  affects the sparsity and SPCA is transformed to PCA when  $\lambda = 0$ . Thus, SPCA-SI is equivalent to PCA-SI. Similarly, PCA-SI offers continual learning ability but the parameters are not sparse.

Then, we explain how the continual learning ability is influenced by  $\gamma_i$  and  $\eta$ . Two extreme cases are given as an example. When  $\gamma_i = 0$  and  $\eta = 1$ , SPCA-SI is equivalent to traditional SPCA and information of previous modes is forgotten catastrophically (similar to Fig. 1b). When  $\gamma_i \rightarrow \infty$  and  $\eta = 0$ , the information of mode  $\mathcal{M}_1$  is completely preserved while the knowledge of subsequent modes is not learned. In other cases, information of different modes is memorized and beneficial to monitor multiple modes simultaneously.

2) *Computational complexity*: The computational complexity focuses on Algorithms 1 and 2.  $k_{total}$  is the total number of iterations. Here we use *flam* to reflect the complexity. The calculation of  $\mathbf{G}_i$  needs  $\frac{1}{2}N_i m^2 + 2m$  flam. For mode  $\mathcal{M}_1$ ,  $10m^2 + 38m + 14$  flam is required for each iteration in Algorithm 1. Thus, the computational complexity is  $(10m^2 + 38m + 14)k_{total} + l(\frac{1}{2}N_1 m^2 + 3N_1 m + 2m)$  flam for training. For mode  $\mathcal{M}_i$  ( $i \geq 2$ ), Algorithm 1 needs  $10m^2 + 50m + 14$  flam in total for each iteration. The training phase needs  $(10m^2 + 50m + 14)k_{total} + l(\frac{1}{2}N_i m^2 + 3N_i m + 2m)$  flam.

## V. CASE STUDY

This section adopts two case studies to illustrate the effectiveness of SPCA-SI. Recursive PCA (RPCA) [27] and improved mixture of probabilistic PCA (IMPPCA) [26] are employed for comparison. For IMPPCA, the mode is automatically identified by membership degree. The fault detection rate (FDR) and false alarm rate (FAR) are employed to evaluate the monitoring performance.

### A. Numerical case

The following numerical case is adopted:

$$\begin{bmatrix} x_1 \\ x_2 \\ x_3 \\ x_4 \\ x_5 \\ x_6 \\ x_7 \\ x_8 \end{bmatrix} = \begin{bmatrix} 0.55 & 0.82 & 0.94 \\ 0.23 & 0.45 & 0.62 \\ -0.61 & 0.62 & 0.41 \\ 0.49 & 0.79 & 0.89 \\ 0.89 & -0.92 & 0.06 \\ 0.76 & 0.74 & 0.35 \\ 0.46 & 0.28 & 0.81 \\ -0.02 & 0.41 & 0.01 \end{bmatrix} \begin{bmatrix} s_1 \\ s_2 \\ s_3 \end{bmatrix} + e$$

where the noise  $e$  follows Gaussian distribution with  $e_i \sim \mathcal{N}(0, 0.001)$ ,  $i = 1, \dots, 8$ . Sequential data are generated successively from two modes:

- Mode 1:  $s_1 \sim \mathcal{U}([-10, -9.7])$ ,  $s_2 \sim \mathcal{N}(-5, 1)$ , and  $s_3 \sim \mathcal{U}([2, 3])$ ;
- Mode 2:  $s_1 \sim \mathcal{U}([-6, -5.7])$ ,  $s_2 \sim \mathcal{N}(-1, 1)$ , and  $s_3 \sim \mathcal{U}([3, 4.2])$ ;

where  $\mathcal{U}([-10, -9.7])$  represents the uniform distribution between  $-10$  and  $-9.7$ , and so on.

We generate 1000 normal samples to train the monitoring model and 1000 samples for fault detection, including the first 500 normal samples and the last 500 faulty samples through the following scenarios:

TABLE I  
COMPARATIVE SCHEME FOR NUMERICAL CASE

	Methods	Training sources	Model label	Testing sources
Situation 1	SPCA	Mode 1	A	Mode 1
Situation 2	SPCA-SI	Model A+Mode 2	B	Mode 2
Situation 3	SPCA-SI	-	B	Mode 1
Situation 4	SPCA	Mode 2	C	Mode 2
Situation 5	SPCA	-	C	Mode 1
Situation 6	RPCA	Modes 1,2	D	Mode 1
Situation 7	RPCA	-	D	Mode 2
Situation 8	IMPPCA	Modes 1,2	E	Mode 1
Situation 9	IMPPCA	-	E	Mode 2

TABLE II  
FDR (%) AND FAR (%) FOR NUMERICAL CASE

Fault type	Fault 1		Fault 2		Fault 3	
	FDR	FAR	FDR	FAR	FDR	FAR
Situation 1	100	7.4	100	2.6	96.8	0
Situation 2	100	6.6	100	2.2	91.0	0
Situation 3	98.6	2.4	99.6	1.0	90.6	4.6
Situation 4	100	8.4	100	2.6	96.4	0
Situation 5	100	93.4	100	90	98.8	65.2
Situation 6	100	98.4	100	98.4	100	98.4
Situation 7	100	33.2	100	100	100	100
Situation 8	100	2.2	100	2.6	95.2	1.4
Situation 9	100	2.2	100	1.8	96.0	2.0

- Fault 1: step fault of  $x_3$ ,  $x_3 = x_3^* + 0.08$ ;
  - Fault 2: step fault of  $x_6$ ,  $x_6 = x_6^* + 0.08$ ;
  - Fault 3: slope drift of  $x_1$ ,  $x_1 = x_1^* + 0.001(k - 500)$ ;
- where  $500 \leq k \leq 1000$ ,  $x_1^*$ ,  $x_3^*$  and  $x_6^*$  are normal.

The simulation scheme is designed to illustrate the effectiveness and superiorities of SPCA-SI, as summarized in Table I. Note that ‘-’ indicates that there is no need to retrain the model and the current monitoring model is adopted for fault detection. The first five situations are utilized to verify that SPCA-SI alleviates the catastrophic forgetting of traditional SPCA and furnishes self-learning ability. Specifically, the results of Situations 1 and 4 testify the effectiveness of SPCA for a mode. The monitoring results of Situations 2 and 3 are used to prove that SPCA-SI is able to monitor two modes simultaneously by a continually updated model, which assimilates new data when a new mode appears. Situation 5 is designed to show that SPCA fails to monitor the previous mode and the learned knowledge is overwritten by new information. For situations 6-9, RPCA and IMPPCA are compared to illustrate the superiorities of SPCA-SI further.

Take Fault 1 as an example to interpret the monitoring consequences in detail, as described in Fig. 2. As the monitoring charts for Mode 1 and Mode 2 are similar for SPCA, the simulation chart of Situation 1 is not listed. In Figs. 2a-2b, SPCA-SI enables to detect the fault in Modes 1 and 2 accurately by model B, which is updated based on the existing model A and data from Mode 2. The model C fails to detect the fault in Mode 1, as depicted in Fig. 2d. The FDR is 100% and FAR is 93.4%, which indicates that the learned knowledge of Mode 1 is forgotten when training the model C (similar to Fig. 1b). According to Situations 1-5, SPCA-SI alleviates the catastrophic forgetting of SPCA and provides self-learning ability for successive modes. For Situation 6-7, RPCA is unable to track the system changes and distinguish the novelty from normality. In Figs. 2g-2h, IMPPCA detects the fault accurately and the FDRs are 100%.

The monitoring results of three faults are summarized in Table II. The analysis aforementioned is equally applied to Fault 2 and Fault 3. Traditional SPCA forgets the significant features of previous modes when training the same model sequentially and fails to deliver prominent performance. SPCA-SI is capable of monitoring two modes simultaneously based on a continually updated model and settles the catastrophic forgetting of SPCA. RPCA fails to distinguish between the

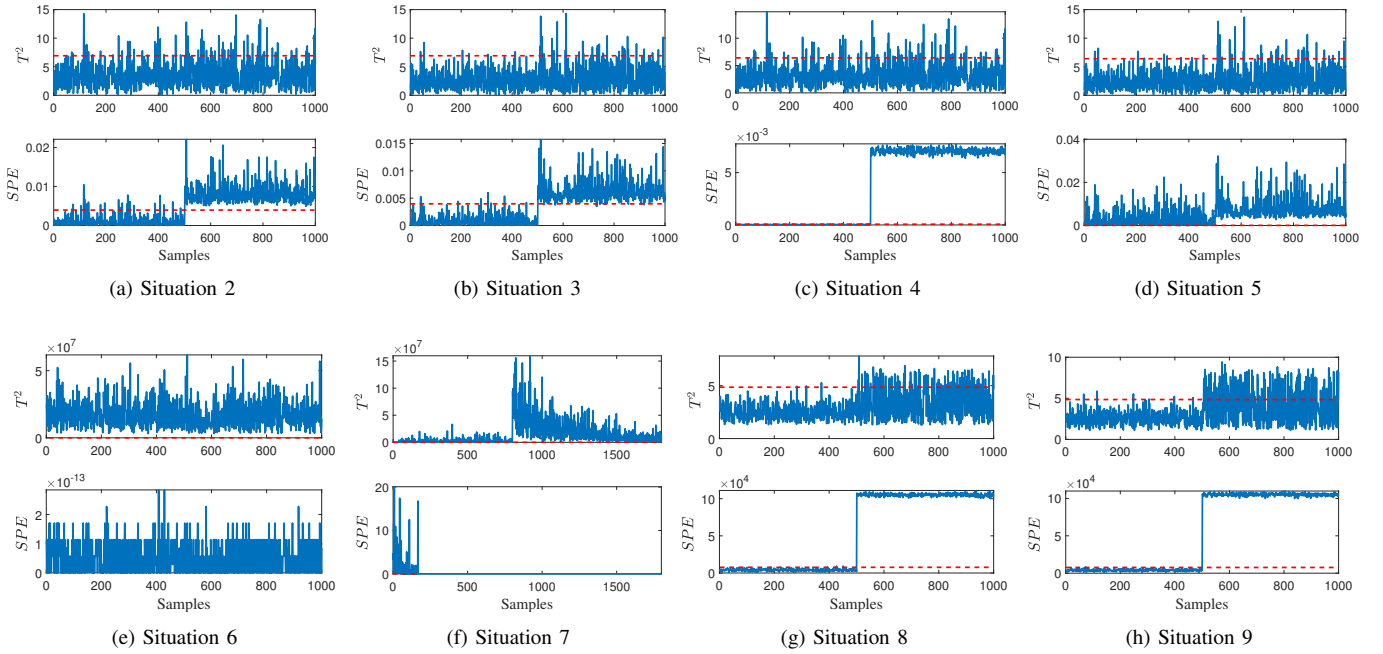


Fig. 2. Monitoring charts of Fault 1

normal modes and faults. IMPPCA detects the fault accurately and needs to be retrained from scratch when new modes appear. Thus, it consumes much more storage space and computational resource than SPCA-SI. Overall, SPCA-SI with self-learning ability is superior to IMPPCA and RPCA, as it can monitor multiple modes accurately, and the computation and storage resources are saved in the long run.

### B. Pulverizing system process monitoring

The 1000-MW ultra-supercritical thermal power plant is increasingly popular due to potential economic benefits and low pollution [10]. This paper investigates the coal pulverizing system in Zhoushan Power Plant in China, which provides high quality pulverized coal for boiler. As depicted in Fig. 3, it contains coal feeder, coal mill, rotary separator, raw coal hopper and stone coal scuttle. In practical systems, the types

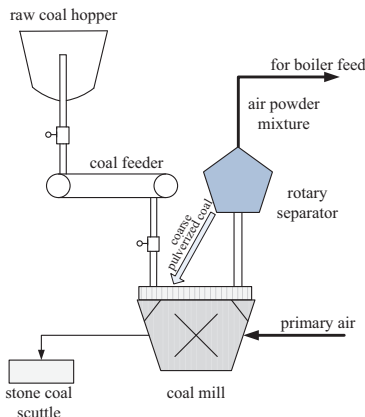


Fig. 3. Schematic diagram of the coal pulverizing system

of coal and unit load would change frequently, thus generating successive operating modes.

In this paper, we focus on two typical faults, namely, abnormality from outlet temperature (Fault 4) and rotary separator (Fault 5). The information is summarized in Table III. Note that the number of training samples and testing samples are shorted for NoTrS and NoTeS, respectively. Nine key variables are selected by prior knowledge. Assume that when new modes appear, the system operates under the normal condition at the preliminary stage.

To illustrate the effectiveness and self-learning ability of SPCA-SI, 17 situations are designed in Table IV. Three different modes are considered in this case. Similar to the numerical case, Situations 1, 4 and 9 are utilized to illustrate the effectiveness of SPCA for a mode. Situations 2, 3, 6, 7 and 8 are designed to verify that SPCA-SI can monitor several modes simultaneously, where new data are assimilated while preserving the learned knowledge. Situations 5, 10 and 11 are employed to show the catastrophic forgetting issue of SPCA. For Situations 12-14, RPCA is adopted to track the successive modes. Take Situation 12 as an example, Modes 1-3 appear sequentially and Mode 1 occurs again, and the fault occurs in Mode 1. For Situations 15-17, IMPPCA is adopted to monitor three modes and the training data are required to be complete.

The monitoring results of Fault 4 and Fault 5 are summarized in Table V. Take Fault 4 as an instance to explain the results detailedly. SPCA can detect the fault in Mode 1 accurately, but the FAR is 5.62%. When a new mode 2 arrives, the model is updated based on the model A and the newly collected data. Thus, the monitoring model B is able to monitor the two successive modes simultaneously, and the FDRs are higher than 99%. Besides, the FAR of Situation 3 is lower than that of Situation 1, which indicates that information of

TABLE III  
DATA INFORMATION OF THE COAL PULVERIZING SYSTEM

Fault type	Mode number	NoTrS	NoTeS	Fault location
Fault 4	1	2160	2880	909
	2	1080	1080	533
	3	1440	1440	626
Fault 5	1	2880	1080	806
	2	720	720	352
	3	2880	2160	134

TABLE IV  
SIMULATION SCHEME FOR THE PULVERIZING SYSTEM

	Methods	Training sources	Model label	Testing sources
Situation 1	SPCA	Mode 1	A	Mode 1
Situation 2	SPCA-SI	Model A+Mode 2	B	Mode 2
Situation 3	SPCA-SI	-	B	Mode 1
Situation 4	SPCA	Mode 2	C	Mode 2
Situation 5	SPCA	-	C	Mode 1
Situation 6	SPCA-SI	Model B+Mode 3	D	Mode 3
Situation 7	SPCA-SI	-	D	Mode 1
Situation 8	SPCA-SI	-	D	Mode 2
Situation 9	SPCA	Mode 3	E	Mode 3
Situation 10	SPCA	-	E	Mode 1
Situation 11	SPCA	-	E	Mode 2
Situation 12	RPCA	Modes 1, 2, 3	F	Mode 1
Situation 13	RPCA	-	F	Mode 2
Situation 14	RPCA	-	F	Mode 3
Situation 15	IMPPCA	Modes 1, 2, 3	H	Mode 1
Situation 16	IMPPCA	-	H	Mode 2
Situation 17	IMPPCA	-	H	Mode 3

Mode 2 is beneficial to reduce the false alarms of Mode 1. The monitoring model C enables to monitor two modes. But the FAR of Mode 1 is 6.5% and higher than that of SPCA-SI. When the new mode 3 appears, the proposed SPCA-SI trains the model D based on the model B and the current data collected. It enables to monitor the three modes simultaneously and the FDRs approach to 100%. Besides, the FARs are the lowest among all situations. It is revealed that SPCA-SI can preserve partial significant information of trained modes, which is advantageous to monitor other similar modes. RPCA fails to detect the fault in three modes and the FARs approximate to 100%. Although IMPPCA is capable of monitoring modes 1 and 2, the FAR for Mode 3 is 41.12%. IMPPCA fails to deliver desired expert level monitoring performance.

Owing to the paper length limitation, we just select 8 representative monitoring charts of Fault 4, as exhibited in Fig. 4. The simulation results of SPCA-SI are mainly listed. Two charts of RPCA and IMPPCA are selected as comparison. The analysis of Fault 4 also applies to Fault 5. Note that the FAR of IMPPCA for Mode 2 is 51.28%.

According to Table IV, SPCA is vulnerable to catastrophic forgetting issue and fails to monitor multiple modes based on the same model. SPCA-SI provides self-learning ability and the model is updated when a new mode arrives, which enables it to monitor multiple modes accurately. Moreover, the learned knowledge of previous modes is preserved continually and the model-sensitive parameters are fewer than PCA. Similar

TABLE V  
FDR (%) AND FAR (%) FOR THE PRACTICAL CASE

Fault type	Fault 4		Fault 5	
	FDR	FAR	FDR	FAR
Situation 1	99.95	5.62	100	0
Situation 2	99.45	0	100	5.98
Situation 3	99.95	4.07	100	0
Situation 4	99.45	0	100	15.38
Situation 5	99.95	6.5	100	0
Situation 6	100	0.32	93.49	0
Situation 7	99.95	1.54	100	0
Situation 8	99.45	0	100	13.96
Situation 9	100	0.48	92.75	0
Situation 10	99.95	75.77	100	0
Situation 11	100	100	100	94.87
Situation 12	100	99.45	100	100
Situation 13	100	100	100	100
Situation 14	100	100	100	100
Situation 15	100	6.61	100	3.23
Situation 16	100	6.95	100	51.28
Situation 17	100	41.12	98.96	0

to numerical case, RPCA is incapable of separating normal modes and faults. Besides, IMPPCA is unable to monitor three modes accurately as the FARs are more than 20%. When a new mode appears, we need to store data and retrain the model from scratch, which costs considerable resources and energy. In conclusion, SPCA-SI outperforms other comparative methods in consideration of detection accuracy and demanding resources in the long term.

## VI. CONCLUSION

This paper presented a novel SPCA-SI method with self-learning ability for monitoring successive modes. The importance measure of variables is evaluated by SI along the learning trajectory. The acquired knowledge of previous modes is accumulated and the model is updated when new data are available, thus delivering excellent performance for successive modes. The optimization issue is settled by APG and the learning rate is adaptively determined to accelerate convergence. Besides, the influence of parameters is discussed and different methods can be converted by specific parameter setting. SPCA-SI furnishes excellent model interpretability, as the critical parameters are sparse. Moreover, a novel  $T^2$  statistic is presented, where the significant information of previous modes is consolidated further. The effectiveness of the proposed method has been illustrated by a numerical case and a practical industrial system.

This proposed method requires the similarity among different modes and prior information about mode switching time. In future, we'll investigate the numerous and diverse modes, with the mode switching time identified automatically.

## REFERENCES

- [1] M. Quiñones-Gruero, A. Prieto-Moreno, C. Verde, and O. Llanes-Santiago, "Data-driven monitoring of multimode continuous processes: A review," *Chemometrics and Intelligent Laboratory Systems*, vol. 189, pp. 56–71, 2019.
- [2] B. Wang, Z. Li, Z. Dai, N. Lawrence, and X. Yan, "Data-driven mode identification and unsupervised fault detection for nonlinear multimode processes," *IEEE Transactions on Industrial Informatics*, vol. 16, no. 6, pp. 3651–3661, 2020.

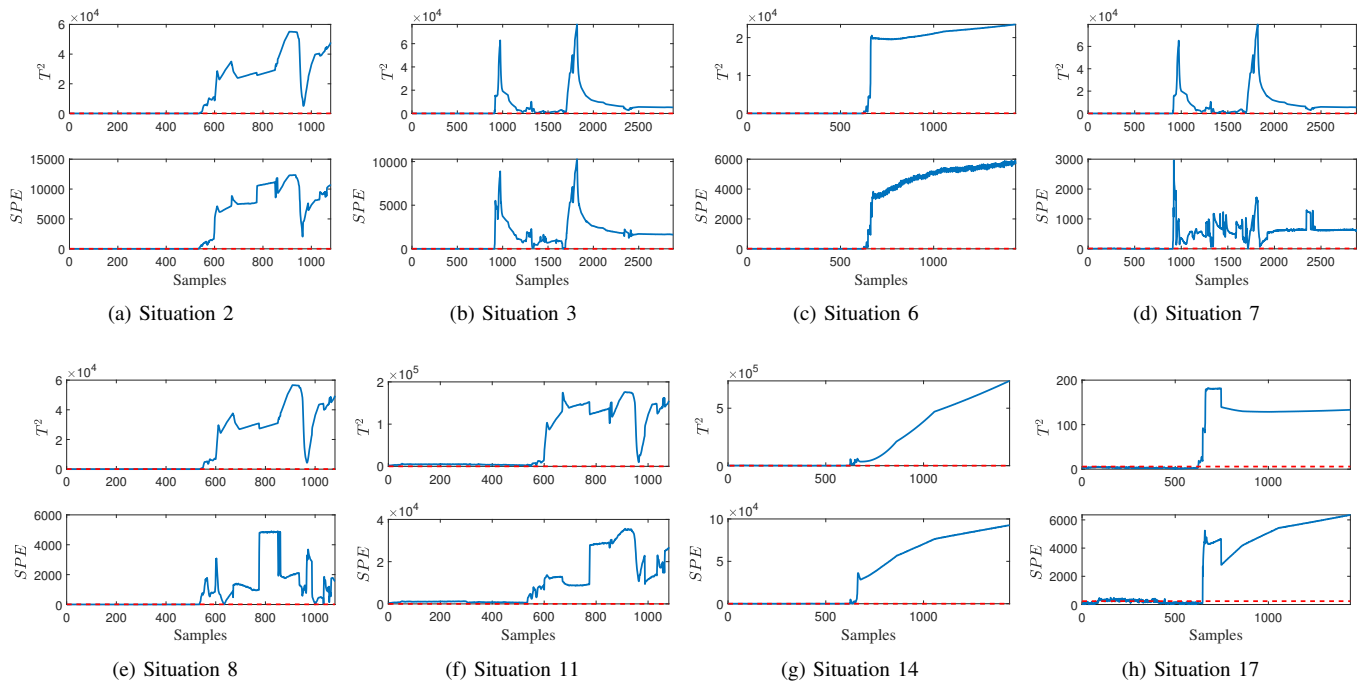


Fig. 4. Monitoring charts of Fault 4

- [3] K. Zhang, K. Peng, and J. Dong, "A common and individual feature extraction-based multimode process monitoring method with application to the finishing mill process," *IEEE Transactions on Industrial Informatics*, vol. 14, no. 11, pp. 4841–4850, 2018.
- [4] L. Zhou, J. Zheng, Z. Ge, Z. Song, and S. Shan, "Multimode process monitoring based on switching autoregressive dynamic latent variable model," *IEEE Transactions on Industrial Electronics*, vol. 65, no. 10, pp. 8184–8194, 2018.
- [5] Y. Liu, J. Zeng, J. Bao, and L. Xie, "A unified probabilistic monitoring framework for multimode processes based on probabilistic linear discriminant analysis," *IEEE Transactions on Industrial Informatics*, vol. 16, no. 10, pp. 6291–6300, 2020.
- [6] Y. Jiang and S. Yin, "Recent advances in key-performance-indicator oriented prognosis and diagnosis with a MATLAB toolbox: DB-KIT," *IEEE Transactions on Industrial Informatics*, vol. 15, no. 5, pp. 2849–2858, 2019.
- [7] J. Zhang, M. Chen, H. Chen, X. Hong, and D. Zhou, "Process monitoring based on orthogonal locality preserving projection with maximum likelihood estimation," *Industrial & Engineering Chemistry Research*, vol. 58, no. 14, pp. 5579–5587, 2019.
- [8] X. Peng, Y. Tang, W. Du, and F. Qian, "Multimode process monitoring and fault detection: A sparse modeling and dictionary learning method," *IEEE Transactions on Industrial Electronics*, vol. 64, no. 6, pp. 4866–4875, 2017.
- [9] J. Shang, D. Zhou, M. Chen, H. Ji, and H. Zhang, "Incipient sensor fault diagnosis in multimode processes using conditionally independent bayesian learning based recursive transformed component statistical analysis," *Journal of Process Control*, vol. 77, pp. 7–19, 2019.
- [10] J. Zhang, D. Zhou, and M. Chen, "Monitoring multimode processes: a modified PCA algorithm with continual learning ability," *arXiv:2012.07044*, 2020.
- [11] J. Kirkpatrick, R. Pascanu, N. Rabinowitz, J. Veness, G. Desjardins, A. A. Rusu, K. Milan, J. Quan, T. Ramalho, and A. Grabska-Barwinska, "Overcoming catastrophic forgetting in neural networks," *Proceedings of the National Academy of Sciences of the United States of America*, vol. 114, no. 13, pp. 3521–3526, 2017.
- [12] R. Aljundi, K. Kelchtermans, and T. Tuytelaars, "Task-free continual learning," in *2019 IEEE/CVF Conference on Computer Vision and Pattern Recognition*, 2019, pp. 11 254–11 263.
- [13] R. Hadsell, D. Rao, A. A. Rusu, and R. Pascanu, "Embracing change: Continual learning in deep neural networks," *Trends in Cognitive Sciences*, vol. 24, no. 12, pp. 1028–1040, 2020.
- [14] J. Yoon, E. Yang, J. Lee, and S. J. Hwang, "Lifelong learning with dynamically expandable networks," in *International Conference on Learning Representations*, 2018.
- [15] X. Xu, H. Yang, C. Lian, and J. Liu, "Self-learning control using dual heuristic programming with global Laplacian eigenmaps," *IEEE Transactions on Industrial Electronics*, vol. 64, no. 12, pp. 9517–9526, 2017.
- [16] F. Ye, K. Chakrabarty, Z. Zhang, and X. Gu, "Self-learning and adaptive board-level functional fault diagnosis," in *The 20th Asia and South Pacific Design Automation Conference*, 2015, pp. 294–301.
- [17] J. Feldmann, N. Youngblood, C. D. Wright, H. Bhaskaran, and W. H. P. Pernice, "All-optical spiking neurosynaptic networks with self-learning capabilities," *Nature*, vol. 569, no. 7755, pp. 208–214, 2019.
- [18] J. Zhang, D. Zhou, and M. Chen, "Monitoring nonstationary processes based on recursive cointegration analysis and elastic weight consolidation," *arXiv:2101.08579*, 2021.
- [19] F. Zenke, B. Poole, and S. Ganguli, "Continual learning through synaptic intelligence," in *Proceedings of the 34th International Conference on Machine Learning*, vol. 70, 2017, pp. 3987–3995.
- [20] N. Y. Masse, G. D. Grant, and D. J. Freedman, "Alleviating catastrophic forgetting using context-dependent gating and synaptic stabilization," *Proceedings of the National Academy of Sciences*, vol. 115, no. 44, pp. E10 467–E10 475, 2018.
- [21] G. M. van de Ven, H. T. Siegelmann, and A. S. Tolias, "Brain-inspired replay for continual learning with artificial neural networks," *Nature Communications*, vol. 11, no. 1, p. 4069, 2020.
- [22] H. Li and Z. Lin, "Accelerated proximal gradient methods for nonconvex programming," in *Proceedings of the 28th International Conference on Neural Information Processing Systems - Volume 1*, ser. NIPS'15. MIT Press, 2015, p. 379–387.
- [23] A. Beck and M. Teboulle, "Fast gradient-based algorithms for constrained total variation image denoising and deblurring problems," *IEEE Transactions on Image Processing*, vol. 18, no. 11, pp. 2419–2434, 2009.
- [24] D. P. Kingma and J. L. Ba, "Adam: A method for stochastic optimization," in *ICLR 2015 : International Conference on Learning Representations 2015*, 2015.
- [25] N. K. Dhingra, S. Z. Khong, and M. R. Jovanovic, "The proximal augmented Lagrangian method for nonsmooth composite optimization," *IEEE Transactions on Automatic Control*, vol. 64, no. 7, pp. 2861–2868, 2019.
- [26] J. Zhang, H. Chen, S. Chen, and X. Hong, "An improved mixture of probabilistic PCA for nonlinear data-driven process monitoring," *IEEE Transactions on Cybernetics*, vol. 49, no. 1, pp. 198–210, 2019.



- [27] W. Li, H. Yue, S. Valle-Cervantes, and S. Qin, "Recursive PCA for adaptive process monitoring," *Journal of Process Control*, vol. 10, no. 5, pp. 471–486, 2000.